

sulfur rings may be stable around Jupiter simultaneously and the emission in each activated by independent, and perhaps nonequilibrium, processes. This possibility is given some credibility by the relative thinness of the ring ($\approx 0.3 R_J$) observed on the first night. If the ring on this night had been composed of hot, newly ionized material, it would have been expected to be substantially thicker (about $2 R_J$), corresponding to the $\pm 10^\circ$ of magnetic latitude traversed by Io in a Jovian rotation (24).

CARL B. PILCHER

Institute for Astronomy, University of Hawaii, Honolulu 96822

References and Notes

1. R. A. Brown, *Int. Astron. Union Symp. No. 65* (1974), pp. 527-531; for additional references see C. B. Pilcher and W. V. Schempp, *Icarus* **38**, 1 (1979).
2. L. Trafton, *Nature (London)* **258**, 690 (1975).
3. I. Kupo, Y. Mekler, A. Eviatar, *Astrophys. J.* **205**, L51 (1976).
4. C. B. Pilcher and J. S. Morgan, *Science* **205**, 297 (1979).
5. A. L. Broadfoot *et al.*, *ibid.* **204**, 979 (1979).
6. D. L. Judge, R. W. Carlson, F.-M. Wu, V. G. Hartmann, in *Jupiter*, T. Gehrels, Ed. (Univ. of Arizona Press, Tucson, 1976), pp. 1068-1101.
7. H. S. Bridge, J. W. Belcher, A. J. Lazarus, J. D. Sullivan, R. L. McNutt, F. Bagenal, J. D. Scudder, E. C. Sittler, G. L. Siscoe, V. M. Vasylunas, C. K. Goertz, C. M. Yeates, *Science* **204**, 987 (1979).
8. R. A. Brown, *Astrophys. J.* **206**, L179 (1976); D. E. Osterbrock, *Astrophysics of Gaseous Nebulae* (Freeman, San Francisco, 1974).
9. Y. Mekler and A. Eviatar, *J. Geophys. Res.* **82**, 2809 (1977).
10. C. B. Pilcher, *Bull. Am. Astron. Soc.* **10**, 579 (1978); J. S. Morgan and C. B. Pilcher, *ibid.*, p. 579.
11. C. B. Pilcher and J. S. Morgan, *Astrophys. J.*, in press.
12. A. J. Dessler and T. W. Hill, *ibid.* **227**, 664 (1979).
13. R. A. Brown, *ibid.* **224**, L97 (1978).
14. J. T. Trauger, G. Münch, F. L. Roesler, *ibid.*, in press.
15. A. Eviatar, G. L. Siscoe, Y. Mekler, *Icarus* **39**, 450 (1979).
16. D. B. Nash, *Eos Trans.* **60**, 307 (1979).
17. The use of R_J here and throughout this report refers to the equatorial radius of the planet.
18. The value $i = 10.6^\circ$ for a ring in the magnetic equator is taken from the Jovian magnetic field model of E. J. Smith, L. Davis, Jr., D. E. Jones, P. J. Coleman, Jr., D. S. Colburn, P. Dyal, and C. P. Sonnett [*J. Geophys. Res.* **79**, 3501 (1974)]. The 9° of planetary rotation during an exposure introduced negligible smearing of the images. The nonzero declination of the earth was taken into account in the preparation of the illustrations. At the time of the observations, the rotation axis of the planet was tilted 14° to the celestial north-south direction. This has been ignored for illustrative purposes.
19. *Sci. News* **116**, 155 (1979).
20. G. L. Siscoe, *J. Geophys. Res.* **82**, 1641 (1977).
21. T. W. Hill and F. C. Michel, *ibid.* **81**, 4561 (1976).
22. T. W. Hill, A. J. Dessler, F. C. Michel, *Geophys. Res. Lett.* **1**, 19 (1974).
23. Y. L. Yung, personal communication.
24. G. L. Siscoe and C.-K. Chen, *Icarus* **31**, 1 (1977).
25. The background for observations to the west of the planet is less uniform than for observations to the east because of asymmetric scattering in the telescope.
26. I thank S. Wolff for her lucid thinking at an altitude of 4200 m, and S. Kawamura, E. Enos, and C. Lai for their dedicated work on the design and construction of the instrumentation. A. N. Stockton provided invaluable assistance in mounting the image tube on the new apparatus. A. J. Dessler and G. L. Siscoe helped to guide me through the magnetospheric literature and provided many useful insights. Supported in part by NASA grant NGL 12-001-057.

9 August 1979; revised 12 October 1979

Tectonic Tilt Rates Derived from Lake-Level Measurements, Salton Sea, California

Abstract. Tectonic tilt at the Salton Sea was calculated by differencing lake-level measurements from two points on the sea. During the past 26 years, tilting was down toward the southeast. By 1970 differential vertical movement amounted to 110 millimeters between two gages situated 38 kilometers apart on the southwest shore. A reversal in tilt direction in late 1972 has diminished the net differential vertical movement to 60 millimeters.

The discovery by Castle *et al.* (1) of significant vertical aseismic tectonic movement over a large region of southern California has led to an examination of records of the vertical geodetic control and a search for other types of geophysical data in order to independently measure and monitor crustal movement in California. Toward this end, we examined records of surface water levels on the Salton Sea taken over the past 26 years.

The Salton Sea occupies the lowest part of the Salton depression, an inland continuation of the Gulf of California (Fig. 1). The altitude of the surface of the Salton Sea is currently about 70 m below sea level. Seasonal lake-level fluctuations are about 0.7 m.

The Salton depression is a large, northwest-trending sedimentary basin that has both downwarped and downfaulted during the late Cenozoic. The

greatest thickness of fill in the basin appears to lie about 75 km south of the Salton Sea near the international border, where an estimated thickness of at least 6.4 km of sediments overlies the basement rock. The depth to a Pliocene seismic refractor is estimated to be 4.7 km. The dip of the basement rock under the Salton Sea is down to the southeast (2).

The shoreline of a Pleistocene lake that lay along the southwest side of the depression near the international border is reported to have been deformed down to the southeast resulting in a 35-m elevation change over a 24-km littoral distance ($1460 \mu\text{rad}$ of tilt) (3). This geophysical and geological evidence suggests that the location of greatest subsidence lay south of the Salton Sea, and that the location of the present lake-filled depression is a result of closure by deltaic sedimentation and not closure by a greater rate of tectonic subsidence.

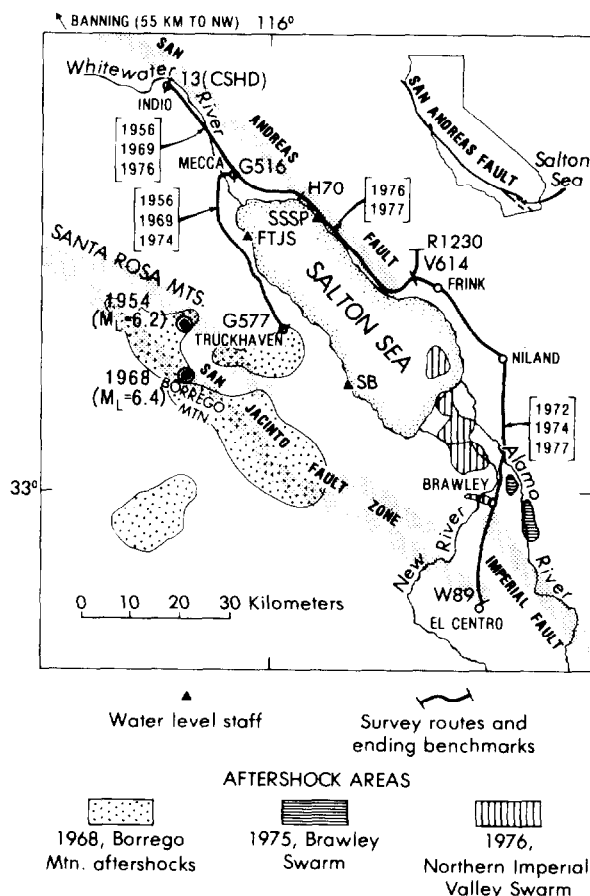


Fig. 1 Map of the Salton Sea area, southern California, showing routes of repeated first-order leveling and locations of terminal benchmarks [13(CSHD), G516, H70, R1230, V614, W89, and G577]. Years in brackets indicate the dates of leveling. The water-level staffs are located at Fig Tree John Springs (FTJS), Salton Sea State Park (SSSP), and Sandy Beach (SB). Locations of the aftershock areas of the 1968 Borrego Mountain earthquake are adapted from Hamilton (9). Locations of the 1975 Brawley swarm area are from Johnson and Hadley (10), and locations of the 1976 Northern Imperial Valley swarm are from Schnapp and Fuis (11); $M_L = 6.2$ and $M_L = 6.4$ are Richter magnitudes for moderate-size earthquakes during the years indicated.

The Salton depression is traversed by active, northwest-trending, strike-slip faults of the San Andreas system. The locations of major fault zones and epicenters of moderate-sized earthquakes within the last 26 years are shown in Fig. 1. The San Jacinto and Imperial fault zones in this region are characterized by considerable seismicity. The San Andreas fault zone in this region, however, is aseismic.

Water-level records have been kept at three sites on the Salton Sea (Fig. 1). Water-level staffs and gages at these

sites are read and maintained by the Imperial Irrigation District (SSSP), the Coachella Valley County Water District (FTJS), and the Water Resources Division of the U.S. Geological Survey (SB). The gage at FTJS is read once each month to the nearest 0.1 foot (30 mm); the gage at SSSP is read to 0.05 foot; and continuous recordings at SB are averaged and reported to the nearest 0.05 foot.

The history of water-level differences between pairs of stations is shown in Fig. 2. The longest historical record is for the

SB-FTJS pair, spaced 38 km apart on the southwest shore (Figs. 1 and 2b). One can clearly recognize in this noisy set of data a trend of down-to-southeast tilting until about 1972, at which time the direction of tilt reversed. To show this trend, we have drawn the curve of a 27-point running average (Fig. 2b). Since 1972, the lake bed has been tilting down to the northwest.

We have attempted to study the timing of changes in the direction or velocity of tilt by plotting the cumulative sum of water-level differences against time as suggested by Wyss (4). The resolution of changes is about 1 year both in the original data (Fig. 1) and in the plot of the cumulative sum (not shown). The rate of tilt appears constant from 1952 to 1967 and averages $0.16 \mu\text{rad}/\text{year}$. From about 1967 to 1970, the tilt rate accelerated to an average of $0.4 \mu\text{rad}/\text{year}$ and then reversed direction in late 1972. The rate of tilt after the reversal was also about $0.4 \mu\text{rad}/\text{year}$, but that rate appears to have diminished since 1975.

The record obtained by differencing the FTJS and SSSP records (Fig. 2a) shows no significant tilt along an east-west 14-km separation between these stations from the beginning of the SSSP record in February 1970 to the most recently obtained record in March 1978. The three-station array allows resolution of the true direction of tilt of the lake bed since 1970. The absence of tilt on the FTJS and SSSP records indicates that

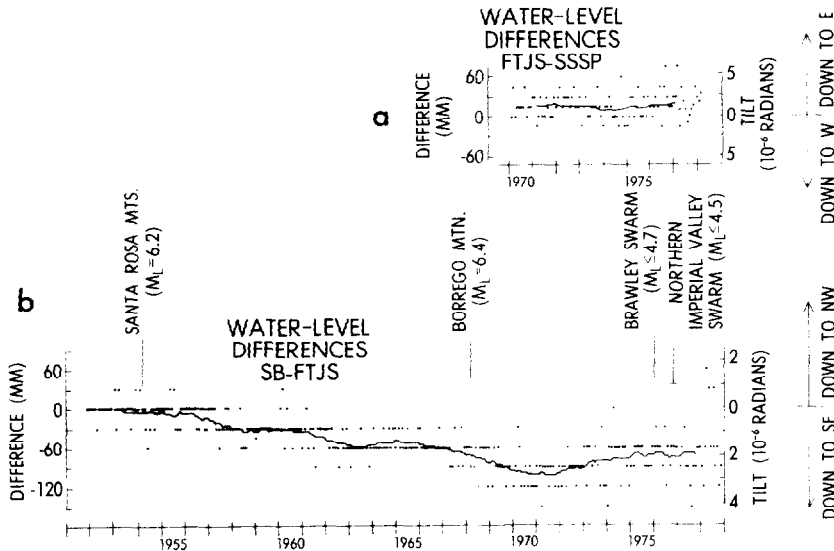


Fig. 2. History of water-level differences between pairs of stations on the Salton Sea. The continuous line is a 27-point running average; (a) water-level differences for the FTJS-SSSP pair; (b) water-level differences between SB and FTJS. Original data are shown as points.

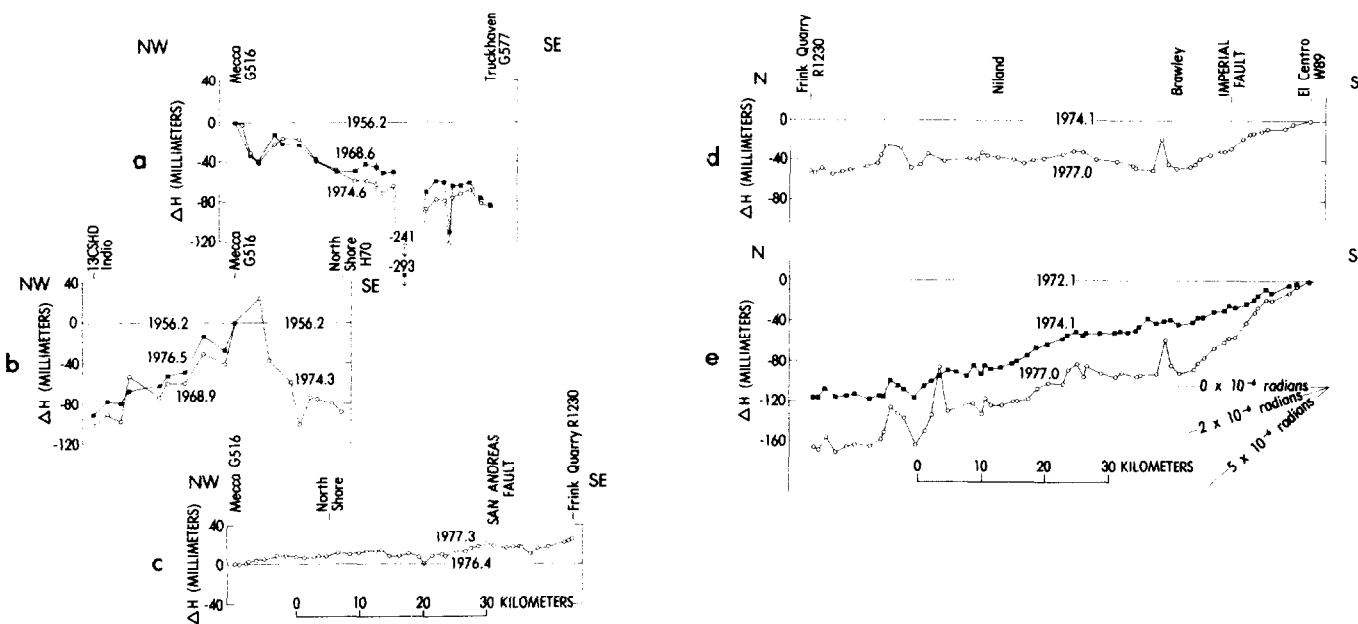


Fig. 3. Profiles of elevation changes (ΔH) from repeated first-order leveling (12). The average date of the level survey (sometimes spanning several months) is shown to the nearest 0.1 year. Profiles in (a), (b), and (c) are referenced to benchmark G516 at Mecca; profiles in (d) and (e) are referenced to benchmark W89 at El Centro. The unconnected points of (a) represent a locally unstable benchmark that has apparently moved more than 190 mm relative to adjacent marks since 1956.2. The tilt scale (in microradians) (lower right) applies to all profiles in this figure.

Table 1. Rates of tectonic tilt (down to southeast) in the Salton depression.

Type of measurement	Period of time (years)	Average tilt rate ($\mu\text{rad}/\text{year}$)
Dip of Pliocene (?) seismic refractor (2)	10^6	≤ 0.02
Deformation of Pleistocene shoreline (3)	10^4 to 10^6	≤ 0.15
First- and second-order geodetic leveling (1902-1928), Banning to Mecca (5)	26	0.34 ± 0.03
First-order leveling (1928-1968), Banning to Mecca (5)	40	0.07 ± 0.02
Water-surface level, Salton Sea (1952-1967)	15	0.1
Water-surface level, Salton Sea (1967-1972)	5	0.4

true tilt has been most recently down to the northwest and is clearly shown by the SB-FTJS record (Fig. 2b).

A nontectonic interpretation of the time history of water-level differences was also considered. A part of the noise on the water-level difference records consists of short-duration tilt of the water surface and subsequent seiching, with a periodicity of about 1.5 hours. High winds must produce considerable seiche amplitudes which decay over several days after the winds die down. This type of noise probably accounts for the few anomalous points on the record (Fig. 2b) that differ from the secular trend by as much as 60 mm.

A curve obtained from a five-point running average (not shown) indicates events having an annual periodicity. These annual events are probably caused by a seasonal buildup of a floating wedge of lower density inflow water at the south end producing as much as 35 mm of temporary tilt of the water surface.

We have considered the possibility that the secular trends in the record could be caused by compaction of sediments, unstable benchmark reference points, or elastic or viscoelastic subsidence of the crust caused by fluctuations of the Salton Sea level since it originally filled in 1905. The timing and magnitude of tilt that could be produced by these processes are not compatible with the record from 1952 to 1978.

Repeated first-order leveling surveys (Fig. 3) encompassing the time of the water-level record are in general agreement with the record (Fig. 2). Figure 3a shows down-to-southeast tilt on a level-survey comparison from 1956.2 to 1968.6 along the south shore of the sea. Lack of tilt between 1968.6 and 1974.6 on the profile in Fig. 3a can be attributed to the tilt reversal in 1972, which apparently erased the tilt accumulated from 1968.6 to 1972. A leveling comparison along the north shore (Fig. 3b) shows a net down-to-southeast tilt of 80 mm from Mecca to North Shore that accumulated between 1956.2 and 1974.3. Associated with this tilt is an apparent 80-mm upward centered at Mecca and a down-to-northwest tilt of the upwarp flank between Mecca and Indio from 1956.2 to 1968.9. Releveling since 1972.1 south of the Salton Sea (Fig. 3, d and e) and since 1976.4 along the northeast shore (Fig. 3e) shows down-to-the-northwest tilting consistent with the water-level record.

Early geodetic leveling and geologic studies give average rates of regional tilting that can be compared to tilt rates de-

rived from the water-level records (Table 1). Two different rates of tilt are apparent. Average tilt rates of less than $0.2 \mu\text{rad}/\text{year}$ typify the long-term geologic average, the geodetic data from 1928 to 1968, and the water-level record from the beginning of record in 1952 until 1967. Average tilt rates greater than $0.3 \mu\text{rad}/\text{year}$ seem to include the two known episodes of more rapid, aseismic vertical deformation that occurred in the period 1906 to 1914 (1, 5) and again in the period since 1959 (1, 6, 7).

In the Salton Sea area, one of these episodes probably began in late 1967 when the water-level record shows a tilt-rate increase from 0.1 to $0.4 \mu\text{rad}/\text{year}$ (Fig. 2). This increased rate was closely followed by the Borrego Mountain earthquake (Richter magnitude $M_L = 6.4$) on 9 April 1968 on the San Jacinto fault (Fig. 1). The reversal of tilt, beginning in late 1972, corresponds in timing with the main development of the southern California uplift in southeastern California (7). We believe that development of the uplift in this region interrupted the previous 16-year trend of down-to-southeast tilting. The data presented here suggest that the first effects of the uplift occurred in 1967, marked by an increase in average tilt rate. Initiation of tilt at this rate may be an indication of an increased strain rate that ultimately triggered the Borrego Mountain earthquake 6 months to 1 year later.

The scale and timing of deformation reported here suggest that there were two kinds of mechanical behavior of the crust in the vicinity of the San Andreas fault. The relatively slow, steady tilt rates of $0.1 \mu\text{rad}/\text{year}$ may be associated with the continuing accumulation of north-south compressive strain, as reported from repeated triangulation and trilateration surveys (8), which generally range from 0.3 to 0.5 microstrain per year. The more rapid tilt rates (greater than $0.3 \mu\text{rad}/\text{year}$) are associated with episodes of rapid aseismic uplift and are probably also associated with increased rates of horizontal strain. The precise

mechanism of these two kinds of deformation along the San Andreas fault system is uncertain.

These observations of water levels in the lake provide a detailed history of vertical aseismic deformation. We wish to point out that these water-level measurements were not designed to monitor crustal deformation. Had the data been collected for this purpose, they could have been read to the nearest 1 mm instead of to 30 mm. The recording of lake water levels either by occasional readings of water-level staff gages or by means of continuous recorders is a straightforward and relatively inexpensive means of obtaining a continuous record of vertical deformation.

MARK E. WILSON*

*U.S. Geological Survey,
Menlo Park, California 94025*

SPENCER H. WOOD

*U.S. Geological Survey, Menlo Park,
and Department of Geology and
Geophysics, Boise State University,
Boise, Idaho 83725*

References and Notes

1. R. O. Castle, J. P. Church, M. R. Elliott, *Science* **192**, 251 (1976).
2. S. Biehler, R. L. Kovach, C. R. Allen, *Mem. Am. Assoc. Pet. Geol.* **3** (1964), p. 126.
3. G. M. Stanley, *Geol. Soc. Am. Spec. Pap.* **87** (1966), p. 165.
4. M. Wyss, *Bull. Seismol. Soc. Am.* **67**, 1091 (1977).
5. S. H. Wood and M. R. Elliott, *Tectonophysics* **52**, 249 (1979).
6. R. O. Castle, M. R. Elliott, J. F. McMillan, R. E. Stone, *Earthquake Notes* **49** (No. 1), 48 (1978).
7. R. O. Castle, M. R. Elliott, S. H. Wood, *Eos* **58**, 495 (1977); R. O. Castle, *Earthquake Inf. Bull.* **10**, 88 (1978).
8. W. Thatcher, *Science* **194**, 691 (1976); J. C. Savage, W. H. Prescott, W. T. Kinoshita, in *Proceedings of the Conference on Tectonic Problems of the San Andreas Fault System*, R. L. Kovach and A. Nur, Eds. (Stanford Univ. Press, Palo Alto, Calif., 1973), pp. 44-53; W. H. Prescott and J. C. Savage, *J. Geophys. Res.* **81**, 4901 (1976).
9. R. M. Hamilton, *U.S. Geol. Surv. Prof. Pap.* **787** (1972), p. 31.
10. C. E. Johnson and D. M. Hadley, *Bull. Seismol. Soc. Am.* **66** (No. 4), 1133 (1976).
11. M. Schnapp and G. Fuis, *U.S. Geol. Surv. Open-File Rep.* **77-431** (1977).
12. Unadjusted first-order leveling data from the National Geodetic Survey (NGS) and the U.S. Geological Survey (USGS): (i) Mecca to Truckhaven: 1956.2 is NGS line L-15875, 1968.6 is NGS line L-21770, 1968.9 is NGS line L-21883, and 1974.6 is NGS line L-23501 and line L-23349; (ii) Indio via Mecca to North Shore: 1956.2 is NGS line L-15875, 1968.9 is NGS line

- L-21170, 1974.3 is NGS line L-23315, and 1976.5 is Riverside County line No. 603; (iii) Mecca to Frink Quarry: 1976.4 is NGS line L-24071, and 1977.3 is USGS Summary Book PV 995U; (iv) Frink Quarry to El Centro: 1972.1 is NGS line 22606, 1974.1 is NGS line L-23243, and 1977.0 is NGS line L-24130.
13. We thank R. O. Castle for encouraging us to study vertical tectonic deformation in southern California; T. C. Hanks and R. A. Page for suggesting that large tilts in the Salton depression, as interpreted from geodetic data, might be manifested in different ways; and B. E. Lofgren for informing us that water-level data were available. We thank R. Spencer and W. Norried of

the Coachella Valley Water District and D. A. Twogood of the Imperial Irrigation District who provided water-level data, S. M. Reese (National Geodetic Survey) who provided recent leveling data, M. R. Elliott who guided us in utilizing the leveling data, and M. J. S. Johnston and J. Ohl who gave helpful suggestions on the data and the manuscript. Publication approved by the Director of the U.S. Geological Survey, 2 January 1979.

* Present address: Cooperative Institute for Research in Environmental Sciences, University of Colorado, Boulder 80309.

17 April 1979; revised 10 October 1979

Dimethyl and Monomethyl Sulfate: Presence in Coal Fly Ash and Airborne Particulate Matter

Abstract. *Dimethyl sulfate and its hydrolysis product monomethyl sulfate have been found at concentrations as high as 830 parts per million in fly ash and in airborne particulate matter from coal combustion processes. This discovery poses a new environmental problem because of the mutagenic and carcinogenic properties of these compounds.*

Much effort and money have been and are being expended to reduce the amount of airborne particulate sulfate generated by fossil-fuel combustion. Most of this activity has occurred because epidemiological studies suggest that long-term, low-level exposure of human populations to the sulfur compounds in airborne particulate matter is detrimental to health. However, the results of these epidemiological studies are still in question, and there has been no demonstration of any long-term toxic effects of any of the sulfur compounds known to be present in airborne particulate matter (1).

We have reported the presence of or-

ganic derivatives or adducts of sulfur oxides in airborne particulate matter collected in urban environments or from coal-burning facilities (2). These unidentified organic derivatives and compounds of sulfur in an oxidation state less than +6 usually account for 5 to 15 percent of the total sulfur present in such samples. The balance of the sulfur is present as salts of SO_4^{2-} , salts of HSO_4^- , or H_2SO_4 . In the process of isolating and identifying the organic derivatives of sulfur oxides, we have found dimethyl sulfate $\{(\text{H}_3\text{CO})_2\text{SO}_2\}$ and its hydrolysis product monomethyl sulfate ($\text{H}_3\text{COSO}_3^-$) to be present in fly ash and in airborne particulate matter originating from coal com-

bustion. To our knowledge, this is the first report of the presence of short-chain alkyl sulfates in the environment except in the vicinity of industrial plants where these compounds are manufactured or used (3). Although these two compounds constitute only about 0.5 percent of the total sulfur present in the samples, we believe this discovery is important because of the proved mutagenic and carcinogenic properties of dimethyl sulfate (4).

Samples of fly ash were collected directly from the flue line (gas temperature $\sim 110^\circ\text{C}$) of a modern chain-grate, stoker type, coal-fired heating plant which burns about 20,000 tons of coal per year. The coal was low-sulfur (0.5 percent), high-ash (14 percent) coal from southern Utah. No size fractionation was attempted on these samples. The plant meets the emissions requirements of the Environmental Protection Agency but has no emission controls except an extended flue line to trap the fly ash and a stack 50 m tall.

We collected the total suspended airborne particulate matter on acid-washed, quartz-fiber filters by using a high-volume sampler with a constant flow controller located on the roof of a building 125 m from the stack and 30 m below the top of the stack. The sampler was operated for from 2 to 5 days to collect each sample during inversion conditions when there was little or no wind. The particulate matter collected was assumed to be emissions from the stack of the heating plant as there were no other major emission sources within 15 km of the plant.

The air particulate and fly ash samples were first extracted in a Soxhlet apparatus with methylene chloride to remove organic materials which interfered with the dimethyl sulfate determination. The fly ash from the flue line was found to contain very low concentrations of organic compounds soluble in methylene chloride and therefore the methylene chloride extraction was omitted. No dimethyl sulfate was extracted from any of the samples with methylene chloride. The samples were then extracted with methanol, some portions by Soxhlet extraction and some in an ultrasonic bath at room temperature (5).

The methanol extracts were analyzed by gas chromatography with a glass capillary column and both a flame ionization detector (FID) and a sulfur-specific flame photometric detector (FPD) (Fig. 1a). Dimethyl sulfate was identified by comparison of the retention time with that of pure dimethyl sulfate standard (Eastman, reagent grade) and by gas chromatography-mass spectrometry (6)

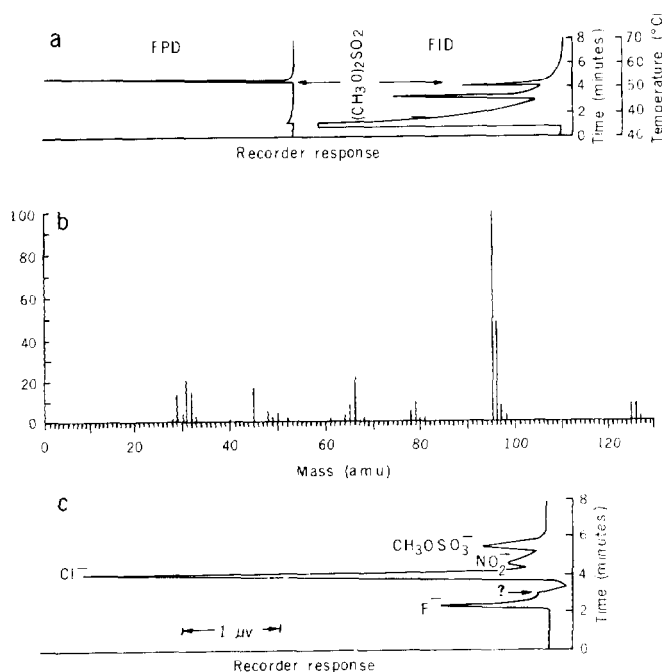


Fig. 1. Data from the methanol extract of fly ash: (a) The FID-FPD gas chromatogram (6). (b) Electron-impact mass spectrum of the peak labeled $(\text{CH}_3\text{O})_2\text{SO}_2$ in (a) (6). (c) Ion chromatogram after the evaporation of methanol followed by dissolution in water (10).